Available online at www.sciencedirect.com
SCIENCE DIRECT®
Cement & Concrete Composites 27 (2005) 141–149
Cement & Concrete Composites
www.elsevier.com/locate/cemconcomp

Flexural behaviour of small steel fibre reinforced concrete slabs

Ali R. Khaloo *, Majid Afshari

Department of Civil Engineering, Sharif University of Technology, Tehran, Iran

Received 16 September 2002; accepted 9 March 2004

Abstract

Influence of length and volumetric percentage of steel fibres on energy absorption of concrete slabs with various concrete strengths is investigated by testing 28 small steel fibre reinforced concrete (SFRC) slabs under flexure. Variables included; fibre length, volumetric percentage of fibres and concrete strength. Test results indicate that generally longer fibres and higher fibre content provide higher energy absorption. The results are compared with a theoretical prediction based on random distribution of fibres. The theoretical method resulted in higher energy absorption than that obtained in experiment. A design method according to allowable deflection is proposed for SFRC slabs within the range of fibre volumetric percentages used in the study. The method predicts resisting moment–deflection curve satisfactorily.

Keywords: Concretes; Cracking; Energy absorption; Fibre reinforcement; Flexural behaviour; Slabs; Steel fibres; Structural design; Tests

1. Introduction

Fibres considerably reduce brittleness of concrete and improve its mechanical properties. Fibre concrete can be used in structural slabs. These slabs can be used for example in structural ceilings, pedestrian bridges and industrial floors.

In 1980, Ghalib [1] proposed a design method based on ultimate strength criteria for small steel fibre reinforced concrete (SFRC) slabs. This method is based on test results of eight steel fibre reinforced two-way slabs. Since then, no new method has been proposed for designing fibre concrete slabs and ACI committee 544 [2] has recommended the same method for design of slabs with small spans. However, the committee has recommended that this method should not be used for slabs with dimensions larger than those tested by Ghalib.

In 1999, Marti et al. [3] tested circular and square slabs under point loading with continuous simple supports along the perimeter. They also presented some formulations, which estimated the results of their slab tests with specific dimensions. However, they stated that additional tests on slabs with other parameters are required to further verify their proposed formulations.

The objective of this research study was to experimentally determine flexural strength, load–deflection curve and energy absorption of small concrete slabs using various percentages of steel fibres. Influences of fibre length and concrete strength were also investigated. Moreover, presenting a design method based on allowable deflection was the other objective of this study.

2. Research significance

Numerous research studies have been performed on mechanical properties of fibre concrete and concrete structural members reinforced with fibres under various loading conditions. However, studies on behaviour of concrete slabs reinforced with fibres considering various parameters are limited.

In the present investigation, influence of percentage and length of fibres on strength and energy absorption of concrete slabs with two different concrete strengths is studied. According to theoretical evaluation, design bases for application are presented.

3. Experimental program

Fourteen concrete mixtures with four different fibre contents, two different fibre lengths and two concrete strengths were designed.

* Corresponding author. Fax: +98-21-601-4828.
E-mail address: khaloo@sharif.edu (A.R. Khaloo).

0958-9465/$ - see front matter © 2004 Elsevier Ltd. All rights reserved.
doi:10.1016/j.cemconcomp.2004.03.004

The slabs were square with dimensions of 820×820 mm and thickness of 80 mm. Four corners of slabs were seated on roller points which provided clear span length of 680 mm. Point load was applied by stroke mode of an actuator on 80×80×10 mm steel plate placed at slab centre. The displacement at the loading point was increased at rate of 1.5 mm/min. Sensitive linear voltage differential transducers were used to measure the deflection at slab centre.

The compressive strengths of 152.4×304.8 mm cylindrical plain specimens were 30 and 45 MPa at the age of 28 days. Details of experimental program are given in Table 1. Mix proportions for the 30 and 45 MPa concretes are presented in Table 2. Similar mixes were used for SFRC specimens. The volumetric percentages of steel fibres, i.e., the ratios of the volume of fibres to the volume of matrix were 0.5, 1.0 and 1.5, which correspond to 25, 50 and 75 kg of steel fibres for mix proportions used in the tests. Cement type I along with river aggregates was used. Sand had a fineness modulus of 2.7 and coarse aggregates had a maximum aggregate size of 19 mm (3/4 in.). The superplasticiser corresponded with ASTM C494 Type F. The crimped shape steel fibres had a rectangular cross-section. Shape properties of steel fibres are given in Table 3.

4. Experimental results and discussion

The average test results for each pair of slabs are presented in Table 4. Also flexural test results of slabs are shown as load–deflection and absorbed energy–deflection curves in Fig. 1a–e.

4.1. Ultimate strength of slabs and energy absorption characteristics

Presence of steel fibres in concrete did not significantly influence the ultimate strength of slabs. Small variation in the ultimate strength was due to changes in compressive strength of concrete caused by addition of fibres. Essentially, ultimate strength corresponds to initiation of

Table 1
Experimental program

Concrete strength (f'_c, MPa)	Fibre type	Fibre volumetric percentage	Specimen number	Number of cylindrical specimens	Number of slabs
30	–	0	1	3	2
	jc25	0.5	2	3	2
		1.0	3	3	2
		1.5	4	3	2
	jc35	0.5	5	3	2
		1.0	6	3	2
		1.5	7	3	2
45	–	0	8	3	2
	jc25	0.5	9	3	2
		1.0	10	3	2
		1.5	11	3	2
	jc35	0.5	12	3	2
		1.0	13	3	2
		1.5	14	3	2
Total number of specimens				42	28

Table 2
Mix proportions of concrete (m^{-3})

Concrete strength (MPa)	Cement (kg)	Fine aggregates (kg)	Coarse aggregates (kg)	Water (kg)	Superplasticiser	Water–cement ratio
30	400	800	1000	192	0.5% = 2 kg	0.48
45	450	750	1000	166.5	1.5% = 6.75 kg	0.37

Table 3
Shape properties of steel fibres

Fibre type	Length (L, mm)	Width (W, mm)	Thickness (T, mm)	Equivalent diameter (d_f, mm)	Aspect ratio (L/d_f)
jc25	25	0.8	0.35	0.597	41.9
jc35	35	1.0	0.35	0.668	52.4

Table 4
Test results

Specimen number	Concrete strength (f'_c, MPa)	Ultimate load (F_{max}, KN)	Deflection at F_{max} (mm)	Energy absorption at F_{max} (J)	Ultimate deflection (mm)	Total energy absorption (J)
1	30.0	22.1	0.52	6.1	0.52	6.1
2	32.2	21.3	0.40	6.0	12.50	78.5
3	31.6	20.2	1.50	21.0	21.00	129.0
4	30.4	22.4	0.70	8.8	23.00	192.4
5	32.4	18.4	0.22	2.2	18.50	73.0
6	33.1	23.2	0.52	8.1	33.00	172.0
7	33.0	22.4	0.95	12.2	28.00	170.5
8	44.9	26.9	0.37	6.2	0.37	6.2
9	47.6	28.0	0.42	7.0	2.75	24.1
10	45.7	34.6	0.40	7.4	23.00	166.6
11	43.7	32.4	1.25	28.1	30.50	335.2
12	45.5	25.0	0.46	7.1	17.50	94.5
13	48.3	27.2	0.78	11.7	20.50	169.8
14	45.9	33.8	0.85	17.8	36.05	372.0

major cracks. The fibres did not considerably influence flexural characteristics of slabs prior to cracking.

The main effect of fibres is on energy absorption capacity that is dealt with in this study. Steel fibres increased energy absorption capacity as measured by the area under load–deflection curve. Also, increase in fibre content decreased the growth rate of total energy absorption (Table 4).

As is shown in Fig. 1b, for jc35 fibres with concrete strength of 30 MPa, increase in fibre volume from 1% to 1.5% did not influence energy absorption of the SFRC slab. In specimens with 0.5% fibre volume, a sudden drop in load–deflection curve is observed which is more pronounced for higher strength concrete (Fig. 1c). Steel fibres of 0.5% did not enhance the behaviour of concrete slabs significantly.

Fibres had similar effects on behaviour of slabs with different concrete strengths. As an average, the energy absorption capacity in 0.5% SFRC slabs was about 12 times that of plain slabs. Also, the energy absorption of the 1.0% SFRC slabs was about 2 times that of 0.5% SFRC slabs. The energy absorption in slabs with 1.5% fibres was about 1.5 times that of slabs with 1.0% fibres. This clearly shows a marked reduction in the increasing rate of energy absorption by increasing the content of steel fibres.

Generally longer fibres (or fibres with larger aspect ratio) provided slightly higher energy absorption capacity (Fig. 1). In average, the total energy absorption of slabs with jc35 fibres was about 1.2 times that of slabs with jc25 fibres (Table 4).

Increase in concrete strength increased the energy absorption capacity of the SFRC slabs.

4.2. Mode of failure

The slabs did not show any visible cracks prior to ultimate strength. The plain slabs failed suddenly at cracking load without any appreciable deflection warning. The deflection for plain slabs was in the neighbourhood of 0.35–0.55 mm with small energy absorption that was about 6 J. The SFRC slabs experienced appreciable deflection after ultimate load and withstood deflections in the range of 12.5–36 mm, except the slab no. 9 which contained low quantity of short fibres and high strength concrete (deflection of this slab was as low as 2.75 mm at failure). This deflection range corresponds to deflection/span ratio from 1.8% to 5.3%. The SFRC slabs with fibre content of 1.0% and 1.5% failed gradually while the fibres were pulled out of concrete. The plain slabs broke in two pieces at ultimate strength, while SFRC slabs maintained their integrity to relatively high deflection after ultimate strength. The failure pattern for plain and SFRC slabs is shown in Fig. 4.

5. Theoretical behaviour of SFRC (after cracking) and flexural analysis

A piece of fibre concrete with unit area ($A = 1$) under pure tension with a monotonically increasing crack opening (u) is considered (Fig. 2) [3]. Assuming that the fibres crossing the section resist tension by bond with concrete, the following initial stress is obtained:

$$\sigma_0 = \rho_f l_f \tau_b / 2 d_f. \quad (1)$$

This equation is based on spatial random distribution of fibres in concrete. ρ_f is volumetric reinforcement ratio, i.e., the ratio of steel fibre weight in one cubic meter of concrete to unit weight of steel. τ_b is bond shear stress that is assumed constant. d_f and l_f are equivalent diameter and length of fibres, respectively.

In Eq. (1), τ_b can be estimated using the following equation:

$$\tau_b = 2 f_{ct} = 0.6 (f'_c)^{\frac{2}{3}}, \quad (2)$$

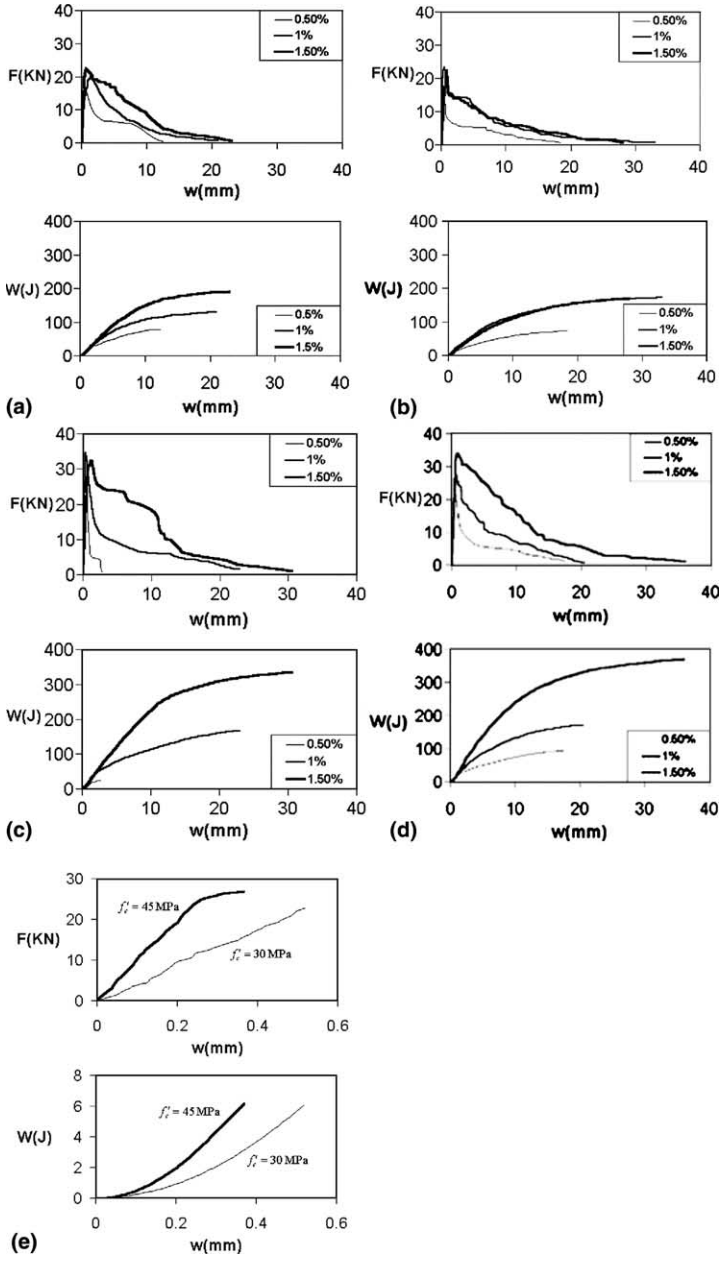

Fig. 1. Load–deflection and absorbed energy–deflection curves for slabs. Concrete strength of (a) 30 MPa and jc25 fibres, (b) 30 MPa and jc35 fibres, (c) 45 MPa and jc25 fibres, (d) 45 MPa and jc35 fibres; and (e) plain concrete slabs.

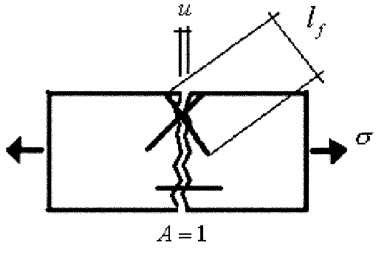

Fig. 2. Pullout of randomly oriented fibres under uniaxial tension.

In which f_{ct} and f'_c are tensile and compressive strength of SFRC at 28 days, respectively. Increase in u, yields the following relationship for stress:

$$\sigma = \sigma_0\left(1 - \frac{2u}{l_f}\right)^2, \quad 0 \leqslant u \leqslant \frac{l_f}{2}. \tag{3}$$

Crack opening parameter ξ, is defined as shown in Fig. 3 [3]. For flexural analysis

$$\theta(h - z) = \xi l_f/2. \tag{4}$$

In Eq. (4), h is section depth, z is compression zone depth and θ is hinge rotation. Based on Eq. (3) and

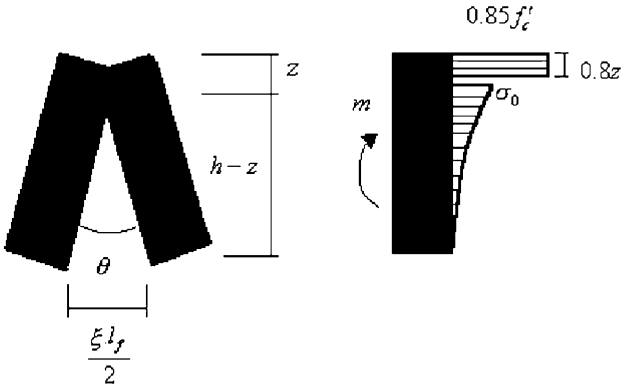

Fig. 3. Rotation and stress distribution at flexural hinge.

stress distribution shown in Fig. 3, compression zone depth (z) and bending moment per unit width (m) are calculated using the following relationships:

For $0 \leqslant \xi \leqslant 1$:

$$z = \frac{h}{1 + \frac{2.04 f_c'}{\sigma_0(3 - 3\xi + \xi^2)}} \quad \text{and}$$

$$m = 0.68 f_c' z \left[0.6z + (h - z) \frac{6 - 8\xi + 3\xi^2}{12 - 12\xi + 4\xi^2} \right]. \tag{5}$$

For $\xi > 1$:

$$z = \frac{h}{1 + \frac{2.04 f_c' \xi}{\sigma_0}} \quad \text{and} \quad m = 0.68 f_c' z \left(0.6z + \frac{h - z}{4\xi} \right). \tag{6}$$

It is required to obtain the relationship between applied load (F) and generated bending moment (m) for the slabs used in present study. Yield line theory is used to analyse the slab shown in Fig. 4 [4,5]. The failure pattern in all the slabs was in the form of a straight line in either north–south or east–west direction (Fig. 4). According to principle of virtual work, the following relations are obtained:

$$\theta = 2\alpha = \frac{4w}{b - a}, \tag{7}$$

$$\sum F\Delta = \sum m\theta l \quad \Rightarrow \quad Fw = m \frac{4w}{b - a}(b + 2c)$$

$$\Rightarrow \quad m = \frac{F(b - a)}{4(b + 2c)}. \tag{8}$$

For the tested slabs, the constants a, b, c and h were 80, 680, 70 and 80 mm, respectively. Substitution of constants a, b, c and h in Eq. (8) yields:

$$F = 5.467m. \tag{9}$$

The Eqs. (4) and (7) result in

$$w = \xi l_f (b - a)/8(h - z). \tag{10}$$

Finally, using Eqs. (5), (6), (9) and (10), the following relationships are obtained:

For $0 \leqslant \xi \leqslant 1$:

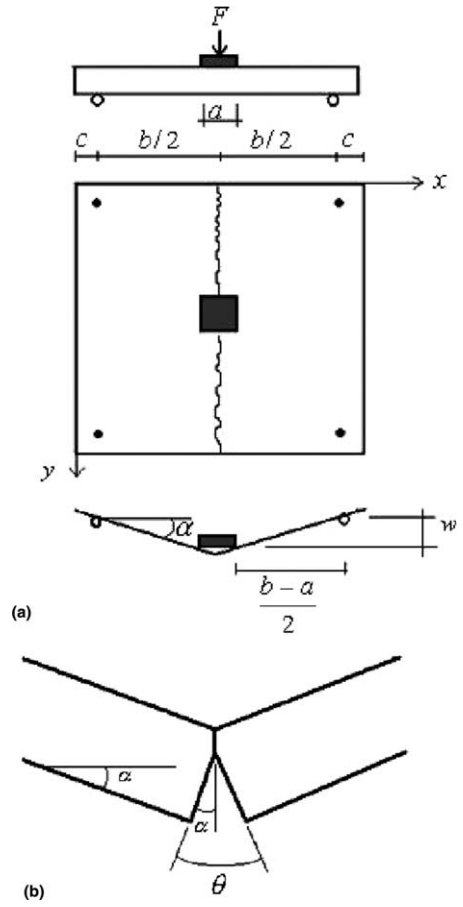

Fig. 4. Analysis of slabs: (a) yield line pattern and (b) flexural hinge.

$$\begin{cases} F = 3.718 f_c' z \left[0.6z + (h - z) \dfrac{6 - 8\xi + 3\xi^2}{12 - 12\xi + 4\xi^2} \right], \\ w = \dfrac{\xi l_f (b - a)}{8(h - z)}. \end{cases} \tag{11}$$

For $\xi > 1$:

$$\begin{cases} F = 3.718 f_c' z \left(0.6z + \dfrac{h - z}{4\xi} \right), \\ w = \dfrac{\xi l_f (b - a)}{8(h - z)}. \end{cases} \tag{12}$$

The value of ξ is arbitrarily changed in order to determine the complete load–deflection (F–w) curve for each slab.

6. Comparison between test results and theory

The theoretical load–deflection curves are compared with experimental results in Fig. 5. Generally, the theoretical predictions are not conservative and present higher energy absorption than actual behaviour. Also as seen in Ref. [3], the theory did not predict some of the test results of Marti et al. satisfactorily.

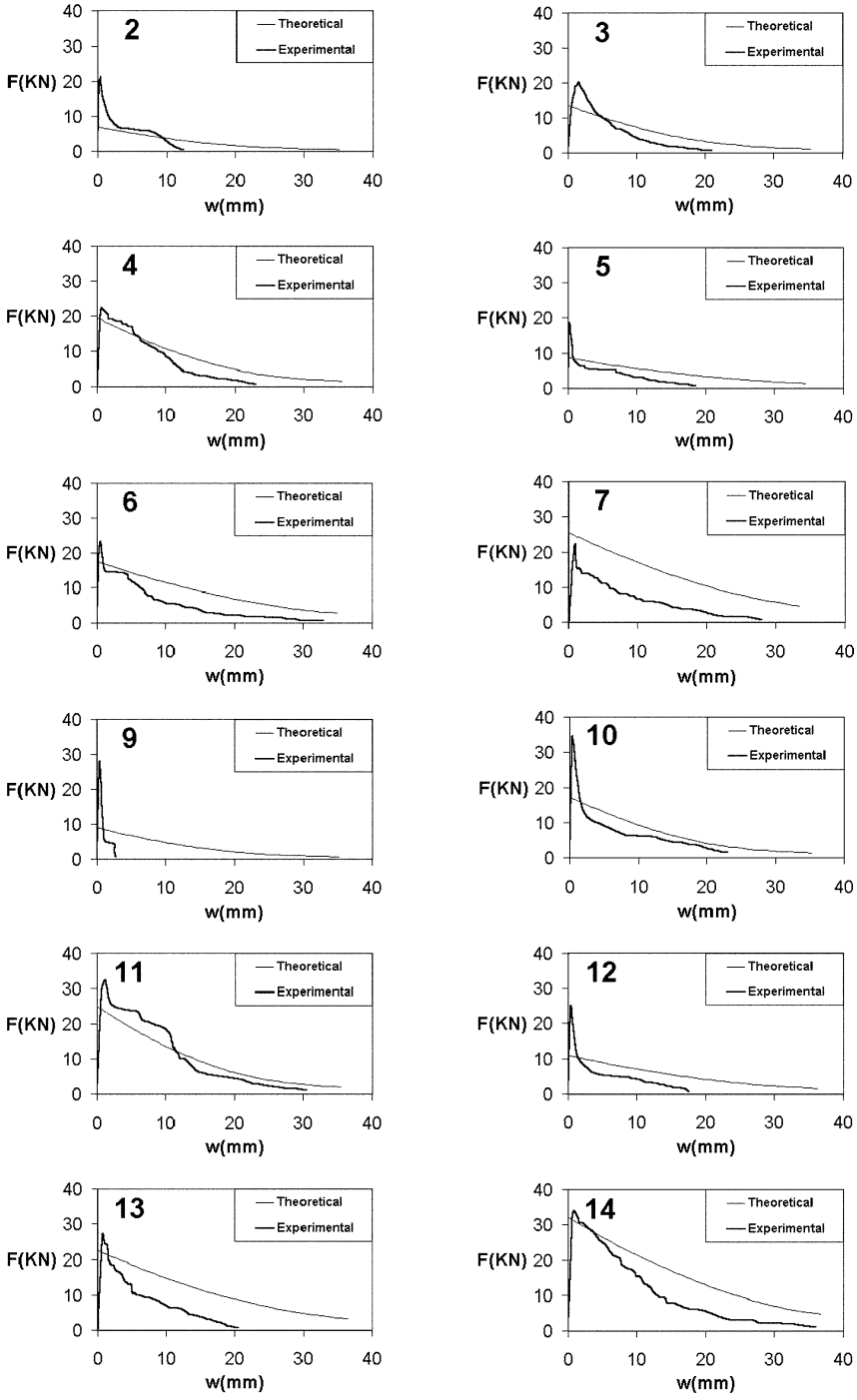

Fig. 5. Comparison between theoretical load–deflection curves and that of experiments (numbers in the top-left of the curves are the specimen numbers).

Three regions in the load–deflection curves are observed. The first region covers the beginning of loading to maximum load that corresponds to cracking of concrete. This region has a high ascending slope. It should be noted that the theory predicts the behaviour of FRC after cracking. The second region begins at cracking load (ultimate load) and ends at a point that the tensile stress is resisted totally by bond between fibres and concrete. This region possesses a high descending slope especially in slabs with low fibre content. Note that this region is a transition state between resisting tension completely by concrete and resisting tension completely by the fibres. The present theory does not predict the test data satisfactorily in the second region. In the third region, the slope of curve reduces and becomes almost parallel to the theoretical curve.

The theoretical prediction is not acceptable for slab no. 9 with strength of 45 MPa and 0.5% of jc25 fibres. Generally, the theory is not justified for concrete with low fibre content (i.e., 0.5% and lower). The prediction considerably overestimates the test data for the slab no. 7 with strength of 30 MPa and 1.5% of jc35 fibres. However, coincidence of theory is relatively good for slab no. 11 with strength of 45 MPa and 1.5% of jc25 fibres.

The loads at deflections of $b/100$ and $b/50$ are presented in Table 5 (panels A and B, respectively). The ratio of load at $w = b/100$ to the ultimate load varies between 0% and 28% in slabs with 0.5% fibre volume (experimental data of column 6 in Table 5, panel A). It is estimated here that about 20% of ultimate load is resisted in slabs with jc25 fibres and about 25% of ultimate load is resisted in slabs with jc35 fibres at deflection of $b/100$. The ratio at $w = b/50$ is 0% in slabs with short fibres and 10% in slabs with long fibres (Table 5, panel B).

The ratio for $w = b/100$ and 1.0% fibre volume has a range of 22–40%. A ratio of about 30% for jc25 fibres and a ratio of about 35% for jc35 fibres are assumed. At $w = b/50$ the variation is within 12% and 19%, in which an average of 15% is assumed here.

In slabs with 1.5% fibre volume the ratio of load at $w = b/100$ to the ultimate load varies between 41% and 65%, where a ratio of 55% is assumed here. At $w = b/50$, this ratio varies between 17% and 27%, where a ratio of 25% is considered.

7. Design recommendation based on allowable deflection

The ratio of theoretical load at maximum test deflection (where the test load vanishes) to theoretical ultimate load (corresponding to $\xi = 0$) for each slab is presented in Table 6. Based on the ratios presented in this table, it is estimated that for fibre percentages of 1.0 and 1.5, when the theoretical load and consequently the theoretical moment reduce to 0.2 of their initial (maximum) value, the test load vanishes. It should be noted that averaging method was found to be suitable to reach at this value. Therefore, that part of theoretical moment–deflection (m–w) curve, which begins at maximum moment (m_0) and ends at $0.2m_0$ will be considered in design (Fig. 6). Deflection w_1 corresponds to $0.2m_0$.

Based on the trend of test results (Fig. 5 and column 7 of Table 5, panels A and B), the theoretical curve is

Table 5
Ratios between load at $w = b/100$ (panel A) and at $w = b/50$ (panel B) and ultimate load

(1) Concrete strength (MPa)	(2) Fibre type	(3) Fibre volumetric percentage	(4) Experimental ultimate load (KN)	(5) Load at $w = b/100$ (KN)		(6) (5)/(4)		(7) Ratio of experimental results to theoretical results (refer to column 5)
				Experiment	Theory	Experiment	Theory	
Panel A								
30	jc25	0.5	21.34	5.9	4.6	0.28	0.22	1.28
		1.0	20.23	7.4	9.1	0.37	0.45	0.81
		1.5	22.44	12.6	13.3	0.56	0.59	0.95
	jc35	0.5	18.39	5.2	6.6	0.28	0.36	0.79
		1.0	23.18	9.3	13.3	0.40	0.57	0.70
		1.5	22.44	9.1	19.7	0.41	0.88	0.46
45	jc25	0.5	27.96	0.0	6.0	0.00	0.21	0.00
		1.0	34.58	7.6	11.7	0.22	0.34	0.65
		1.5	32.37	21.1	16.9	0.65	0.52	1.25
	jc35	0.5	25.02	5.1	8.2	0.20	0.33	0.62
		1.0	27.22	9.3	17.1	0.34	0.63	0.54
		1.5	33.84	21.2	24.6	0.63	0.73	0.86
				Load at $w = b/50$ (KN)				
Panel B								
30	jc25	0.5	21.34	0.0	2.8	0.00	0.13	0.00
		1.0	20.23	2.4	5.6	0.12	0.28	0.42
		1.5	22.44	3.8	8.2	0.17	0.37	0.48
	jc35	0.5	18.39	1.8	4.7	0.10	0.26	0.39
		1.0	23.18	4.4	9.7	0.19	0.42	0.45
		1.5	22.44	5.4	14.5	0.24	0.65	0.37
45	jc25	0.5	27.96	0.0	3.6	0.00	0.13	0.00
		1.0	34.58	5.1	7.1	0.15	0.21	0.72
		1.5	32.37	8.3	10.4	0.26	0.32	0.80
	jc35	0.5	25.02	2.6	5.9	0.10	0.24	0.44
		1.0	27.22	4.4	12.4	0.16	0.46	0.36
		1.5	33.84	9.2	18.0	0.27	0.53	0.51

Table 6
Ratios between theoretical load at maximum test deflection and theoretical ultimate load

Concrete strength (MPa)	Fibre type	Fibre volumetric percentage	Ratio between theoretical load at maximum test deflection and theoretical ultimate load
30	jc25	0.5	0.44
		1.0	0.22
		1.5	0.19
	jc35	0.5	0.42
		1.0	0.18
		1.5	0.25
45	jc25	0.5	0.85
		1.0	0.18
		1.5	0.11
	jc35	0.5	0.44
		1.0	0.38
		1.5	0.15

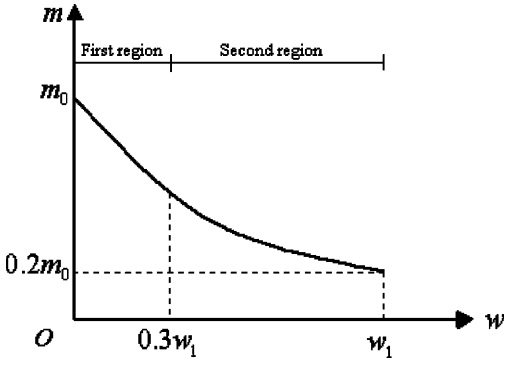

Fig. 6. Proposed moment–deflection curve for SFRC slab design.

divided into two regions. The first region covers deflections from 0 to $0.3w_1$ and the second region covers deflections from $0.3w_1$ to w_1. In the first region the theoretically calculated moment is multiplied by 0.75 and in the second region the calculated moment is multiplied by 0.5. Exertion of these strength reduction factors on theoretical values is recommended for design of SFRC slabs containing 0.75–1.75% of steel fibres.

7.1. Design steps

1. Determination of theoretical moment–deflection curve up to the deflection corresponding to 20% of maximum moment.
2. Dividing the curve into two regions along deflection axis with 0.3 and 0.7 ratios.
3. In the first region (from 0 to 0.3 of maximum deflection) strength reduction factor of 0.75 and in the second region strength reduction factor of 0.5 to theoretical moment is applied.
4. For any permissible deflection the resisting moment will be obtained from corrected theoretical curve and will be compared with external moment.

8. Conclusions

Based on the results of the study presented in the paper, the following conclusions are reached:

1. Addition of fibres does not significantly increase the ultimate flexural strength of SFRC slabs. However, it improves the energy absorption capacity of slabs. The energy absorption of slabs with fibre volume of 0.5% was about 12 times that of plain concrete slabs. The slabs with fibre volume of 1.0% experienced energy absorption of about 2 times that of slabs with 0.5% fibres. In 1.5% SFRC slabs, the energy absorption was about 1.5 times that of slabs with fibre volume of 1.0%.
2. In slabs with low fibre volume (0.5%) the resisting load after cracking was relatively small. The rate of improvement in energy absorption reduced with increase in fibre content. It is recommended to use fibre volumetric percentages in the range of 0.75–1.75. Longer fibres (i.e., fibres with higher aspect ratio) provided higher energy absorption. The energy absorption of jc35 fibres was about 1.2 times that of jc25 fibres. Increase in strength of fibre reinforced concrete enhances the energy absorption capacity. Also, fibres have similar effects on behaviour of slabs with different concrete strengths.
3. According to comparison between experimental load–deflection curves and a theoretical prediction method, a design method based on allowable deflection is developed for SFRC slabs. The method covers volumetric percentages of steel fibres in the range of 0.75–1.75.

Acknowledgements

The support of research committee of Sharif University of Technology in conducting this study is appreciated.

Appendix A

A.1. Design example

Design a square slab with dimensions of 1.0×1.0 m seated on continuously simple supports in all sides with clear span length (b) of 0.92 m, to resist a minimum uniform load of $q = 19$ kN/m^2 with centre deflection of $b/50$. The steel fibre length, equivalent diameter and fibre content are 25 mm, 0.597 mm and 50 kg/m^3, respectively. Concrete has compressive strength (f'_c) of 28 MPa at 28 days. Distribution of fibres is randomly space-oriented in concrete. Neglect the corner effect of slab in the analysis.

A.2. Solution

Based on yield line theory and considering four diagonal cracks extending from the slab center to the slab corners, the following relations hold [5]:

$$m = qb^2/24, \quad \theta = 2w\sqrt{2}/b,$$

$$m = 19,000(0.92)^2/24 = 670 \text{ Nm/m}$$

external moment,

$$b/50 = 920/50 = 18.4 \text{ mm} \quad \text{deflection limitation.}$$

Assuming the slab thickness as $h = 80$ mm, resisting moment corresponding to $w = 18.4$ mm will be calculated as follows:

$$f_{ct} = 0.3(f'_c)^{2/3} = 0.3(28)^{2/3} = 2.766 \text{ MPa},$$

$$\sigma_0 = \rho_f(l_f/d_f)f_{ct} = (50/7850)(25/0.597)(2.766) = 0.738 \text{ MPa},$$

$$\theta(h-z) = \frac{\xi \times l_f}{2} \Rightarrow \frac{2w\sqrt{2}}{920}(80-z) = \frac{\xi \times 25}{2}$$

$$\Rightarrow w = \frac{4065.86\xi}{(80-z)}. \tag{A.1}$$

The value of ξ is changed arbitrarily to obtain the parameters z and m by relations 5 and 6. Finally based on Eq. (A.1), the theoretical moment–deflection curve is obtained as shown in Fig. 7. The curve yields the following moments:

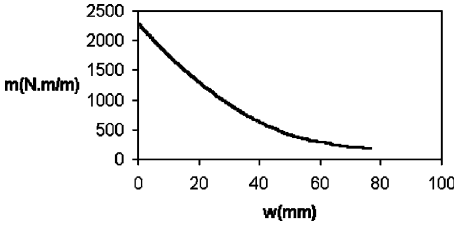

Fig. 7. Theoretical resisting moment–deflection curve for slab of example.

$$m_0 = 2290 \text{ Nm/m} \Rightarrow 0.2m_0 = 458 \text{ Nm/m}.$$

The deflection corresponding to $0.2m_0$ is $w_1 = 47.8$ mm and therefore $0.3w_1$ equals to 14.34 mm. The 18.4 mm deflection falls within the second region. Thus, the theoretical moment should be divided by two to obtain the resisting moment:

$$m_{(w=18.4)} = 1375 \text{ Nm/m},$$

resisting moment $= 1375/2 = 687.5$ Nm/m $>$ 670 Nm/m.

The assumed thickness of 80 mm is acceptable according to the design criterion.

References

[1] Ghalib MA. Moment capacity of steel fibre reinforced small concrete slabs. ACI Journal 1980;(July–August):247–57.
[2] ACI Committee 544 Report, Design Considerations for SFRC, ACI Structural Journal (September–October 1988) (Reapproved 1998) 563–580.
[3] Marti P, Pfyl T, Sigrist V, Ulaga T. Harmonized test procedures for steel fibre-reinforced concrete. ACI Materials Journal 1999;(November–December):676–85.
[4] Jones LL, Wood RH. Yield-Line Analysis of Slabs. London: Thames & Hudson, Chatto & Windus; 1967.
[5] Park R, Gamble WL. Reinforced Concrete Slabs. second ed. John Wiley & Sons; 2000.